THE JOURNAL OF BIOLOGICAL CHEMISTRY VOL. 281, NO. 35, pp. 25241–25249, September 1, 2006
Printed in the U.S.A.

# Increased Sensitivity of Oxidized Large Isoform of Ribulose-1,5-bisphosphate Carboxylase/Oxygenase (Rubisco) Activase to ADP Inhibition Is Due to an Interaction between Its Carboxyl Extension and Nucleotide-binding Pocket*

Received for publication, May 17, 2006, and in revised form, June 22, 2006 Published, JBC Papers in Press, July 5, 2006, DOI 10.1074/jbc.M604756200

**Dafu Wang**[‡] **and Archie R. Portis, Jr.**[‡§1]

*From the* [‡]*Department of Plant Biology, University of Illinois, Urbana, Illinois 61801 and the* [§]*Photosynthesis Research Unit, Agricultural Research Service, United States Department of Agriculture, Urbana, Illinois 61801*

**In *Arabidopsis*, oxidation of the large (46-kDa) isoform activase to form a disulfide bond in the C-terminal extension (C-extension) significantly increases its ADP sensitivity for both ATP hydrolysis and ribulose-1,5-bisphosphate carboxylase/oxygenase (Rubisco) activation, thereby decreasing both activities at physiological ratios of ADP/ATP. In this study, we demonstrate that the C-extension of the oxidized large activase isoform can be cross-linked with regions containing residues that contribute to the nucleotide-binding pocket, with a higher efficiency in the presence of ADP or the absence of nucleotides than with ATP. Coupled with measurements demonstrating a redox-dependent protease sensitivity of the C-extension and a lower ATP or adenosine 5′-*O*-(thiotriphosphate) (ATPγS) affinity of the oxidized large isoform than either the reduced form or the smaller isoform, the results suggest that the C-extension plays an inhibitory role in ATP hydrolysis, regulated by redox changes. In contrast, the ADP affinities of the small isoform and the reduced or oxidized large isoform were similar, which indicates that the C-extension selectively interferes with the proper binding of ATP, possibly by interfering with the coordination of the γ-phosphate. Furthermore, replacement of conserved, negatively charged residues (Asp[390], Glu[394], and Asp[401]) in the C-extension with alanine significantly reduced the sensitivities of the mutants to ADP inhibition, which suggests the involvement of electrostatic interactions between them and positively charged residues in or near the nucleotide-binding pocket. These studies provide new insights into the mechanism of redox regulation of activase by the C-extension in the large isoform.**

Rubisco[2] activase, a nuclear-encoded chloroplast protein, facilitates the conversion of Rubisco from an inactive to active form by releasing tightly bound, inhibitory sugar phosphates from the active site (1). This process requires ATP hydrolysis by activase and is inhibited by ADP (2). Activase belongs to an AAA$^+$ (ATPase associated with diverse cellular activities) protein family, based on sequence homology of its central portion with common AAA motifs, and each monomer contains one nucleotide-binding pocket consisting of residues from Walker A, Walker B, and Sensor 1 domains (1, 3). Site-directed mutagenesis and photoaffinity labeling (4-6) showed that the Walker A motif (G*XXX*GKS; P-loop) is involved in nucleotide binding. A conserved aspartate residue in the Walker B motif (hhhhDE*XX*, h = hydrophobic residue) is involved in metal ligand binding and ATP catalysis (7). The Sensor 1 region has also been implicated in the binding/coordination of ATP (6, 7). Recently, two residues in the Sensor 2 domain were identified as determining specificity for Rubisco (8), in agreement with the involvement of this motif in substrate recognition in other AAA$^+$ members. Several residues in Box VII, which is part of the linkage between the Sensor 1 and Sensor 2 motifs, are essential for maintaining a functional enzyme. Two conserved arginine residues in this region (Arg[237] and Arg[240] in *Arabidopsis*) may act as "arginine fingers" to interact with (or sense the presence of) the γ-phosphate group of ATP bound to an adjacent subunit and induce a conformational change necessary for subsequent ATP hydrolysis (9). A nearby lysine (Lys[243] in *Arabidopsis*) was proposed to coordinate a precise interaction with the γ-phosphate of ATP and to be involved in cooperative interactions between activase subunits (10, 11). This proposal is supported by the involvement of a nearby tryptophan (Trp[246] in *Arabidopsis*) in an ATP-induced increase in the intrinsic fluorescence of activase (12).

Although Rubisco activation requires ATP hydrolysis activity by activase, ATP hydrolysis does not require the presence of Rubisco, and the rate of hydrolysis is not tightly coupled to Rubisco activation (1, 2). To avoid unregulated ATP hydrolysis by the activase, most plants (like *Arabidopsis*) have two isoforms of activase, and the large isoform appears to tightly regulate ATP hydrolysis of both isoforms at physiological ADP/ATP ratios via thioredoxin-mediated redox changes (13, 14).

* This work was supported in part by a grant from the United States Department of Energy (DE-AI02-97ER20268). The costs of publication of this article were defrayed in part by the payment of page charges. This article must therefore be hereby marked "*advertisement*" in accordance with 18 U.S.C. Section 1734 solely to indicate this fact.

[1] To whom correspondence should be addressed. Tel.: 217-244-3083; Fax: 217-244-4419; E-mail: arportis@uiuc.edu.

[2] The abbreviations used are: Rubisco, ribulose-1,5-bisphosphate carboxylase/oxygenase; AAA$^+$, super family of ATPases associated with diverse cellular activities; ATPase, ATP hydrolysis; biotin_PEO, biotinyl-iodoacetamidyl-3,6-dioxaoctanediamine; PEAS, *N*-((2-pyridyldithio)-ethyl)-4-azidosalicylamide; RuBP, D-ribulose-1,5-bisphosphate; ATPγS, adenosine 5′-*O*-(thiotriphosphate); C-extension, C-terminal extension; DTT, dithiothreitol; MALDI-TOF, matrix-assisted laser desorption/ionization-time of flight; Tricine, *N*-[2-hydroxy-1,1-bis(hydroxymethyl)ethyl]glycine.

The two isoforms in *Arabidopsis* and other plants (*e.g.* spinach, barley, rice, and cotton) differ only at the C terminus (15–19). The activities of the oxidized large isoform are more sensitive to ADP inhibition than those of the small isoform, and this sensitivity is decreased when the large isoform is reduced. Two cysteines ($Cys^{392}$ and $Cys^{411}$) in the C-terminal extension (C-extension) are required for redox regulation of activase at physiological ADP/ATP ratios *in vitro* (13) and the capacity for down-regulation of Rubisco under the limiting light *in vivo* (14).

Increased self-association of activase increases its activity (20–22), which is typical of many $AAA^+$ proteins that typically function in an oligomeric ring structure. A connection between redox regulation of activase and monomer-oligomer exchange was proposed, based on the fact that the altered sensitivity to the ADP/ATP ratio of the large isoform via redox treatments is sufficient to regulate the activities of both isoforms when mixed at a 1:1 ratio, although the activity of the smaller isoform itself is not altered by redox treatments (23). Recently, an effort to better understand the subunit interactions of activase was made by using mutants containing an introduced cysteine(s) near the N and/or C terminus of the small isoform of cotton activase and homobifunctional sulfhydryl-reactive cross-linkers (24). The N and C termini of the small isoform, which is 40 amino acids shorter than the large isoform in cotton, were shown to be in close proximity. Moreover, cross-linking of the mutants enhanced their activity. However, no cross-linking was observed between the mutants and the wild type large isoform (24).

Several key photosynthetic enzymes in the chloroplast stroma besides activase are regulated by thioredoxin (25), and the molecular basis for regulation is provided by their structures. However, due to the lack of structural information for activase, the molecular details of how the C-extension confers redox regulation of its activity remain unclear. A hypothetical model (23) proposes that oxidation of a disulfide bond between $Cys^{392}$ and $Cys^{411}$ causes a conformational change in the C-extension that allows docking near or into the ATP-binding site(s) and thus hinders the proper binding of ATP. Here we provide support for this hypothesis by studies of the effects of site-directed mutagenesis of several negatively charged residues in the C-extension, redox-dependent changes in proteolytic sensitivity of this region, and cross-linking/peptide mapping.

## EXPERIMENTAL PROCEDURES

*Materials*—1-Anilinonaphthalene-8-sulfonic acid and *N*-((2-pyridyldithio)-ethyl)-4-azido salicylamide (PEAS) were purchased from Molecular Probes (Eugene, OR). Biotinyl-iodoacetamidyl-3,6-dioxaoctanediamine (biotin_PEO) and immobilized, monomeric avidin-agarose were obtained from Pierce. ATPγS was obtained from Roche Applied Science. α-Cyano-4-hydroxycinamic acid and biotin were purchased from Sigma. Sequencing-grade trypsin was purchased from Promega (Madison, WI). Thrombin was obtained from Novagen (Madison, WI). C18 Zip-tips and polyvinylidene difluoride membranes were obtained from Millipore (Bedford, MA).

*Site-directed Mutagenesis, Protein Expression, and Purification*—Site-directed mutagenesis and amino acid insertion were performed using a cDNA clone of the large (46-kDa) isoform of *Arabidopsis* Rubisco activase and the QuikChange® kit from Stratagene (La Jolla, CA). All mutations were confirmed by DNA sequencing. Six single mutations and two double mutations at negatively charged residues were made: E390A, D394A, E398A, D401A, D407A, D408A, E390A/D401A, and D394A/E398A. A new cysteine residue was inserted at position 402 ($C402^{INS}$).

*Protein Expression and Purification*—The recombinant activases and thioredoxin-f were expressed and purified as reported previously (13, 24). Isolation of native Rubisco was performed as reported previously (26).

*Enzyme Activities*—ATP hydrolysis activity of activase at different ADP/ATP ratios was determined by measuring the formation of inorganic phosphate from ATP as reported previously (13). ATP hydrolysis in the absence of ADP was measured by coupling ADP production to NADH oxidation (26). In the presence of ADP, the single step Rubisco activation assay was performed as reported previously (13). In the absence of ADP, activation of the inactive Rubisco-RuBP complex by activase was measured by following 3-phosphoglyceric acid production in a coupled spectrophotometric assay (27). Total Rubisco activity was assayed after preincubation of the inactive Rubisco-RuBP complex with 15 mM $NaHCO_3$ and 15 mM $MgCl_2$ at room temperature for 15 min.

*Nucleotide Binding Assay*—Estimations of nucleotide binding using measurements of fluorescence quenching with 1-anilinonaphthalene-8-sulfonic acid were performed as reported previously (28). Assays of binding using intrinsic fluorescence were performed as reported previously (21). The $K_m$ for ATP hydrolysis of activase was estimated as described (27).

*Limited Proteolysis*—Redox treatments of the recombinant large (46-kDa) *Arabidopsis* activase were performed as reported previously (13). Reduced or oxidized activase was incubated with thrombin (29) at a ratio of 1/100 (w/w) in 50 mM HEPES and 20 mM KCl, pH 7.8. At each indicated time point, an aliquot of the hydrolysate was mixed with 2× SDS sample buffer, boiled immediately, and analyzed by 12% SDS-PAGE. A 48-kDa control protein (Novagen) was used to examine the effect of reduction and oxidation conditions on the performance of thrombin.

*Chemical Cross-linking of the $C402^{INS}$ Mutant*—The derivatization of activase with PEAS was performed as reported previously with some minor modifications (30–32). The $C402^{INS}$ activase (2 mg/ml) was first incubated with 1 mM PEAS in a reaction buffer containing 50 mM HEPES (pH 7.6) and 20 mM KCl at 4 °C in the dark for at least 2 h. For cross-linking in the presence of wild type small (43-kDa) isoform activase, the derivatized $C402^{INS}$ was first passed through a Sephadex G-50 spin column into reaction buffer to remove excess PEAS before mixing with an equal amount of the small isoform activase. The samples were then mixed with 4 mM $MgCl_2$ only or 4 mM $MgCl_2$ plus 0.2 mM nucleotides (ADP or ATP) for 15 min before being transferred onto a prechilled 96-well plate. Cross-linking was initiated with long wave UV light by placing a hand-held UV source (model UVL-21 Blak-Ray® lamp, Ultraviolet Products,

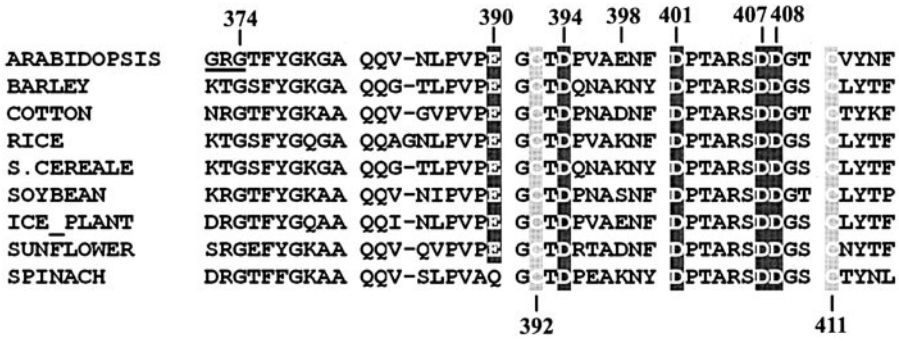


FIGURE 1. **Sequence alignment of the carboxyl extension of the large 46-kDa isoform of activase.** Five conserved Glu and Asp residues (except Glu$^{398}$) are shaded in *dark gray*. The two conserved Cys residues (Cys$^{392}$ and Cys$^{411}$) are shaded in *light gray*. Amino acids are numbered based on the mature sequence of *Arabidopsis* activase as confirmed by N-terminal sequencing (data not shown). The *underlined sequence* ($^{372}$GRG$^{374}$) is the thrombin proteolysis site.

San Gabriel, CA) directly onto the 96-well plate. UV exposure times were indicated.

*Peptide Derivatization and Purification*—The steps for identification of peptides cross-linked with the C-extension were modified from previous reports (30, 32) and are outlined in Fig. 5*D*. PEAS-derivatized and cross-linked C402$^{INS}$ activase (Steps 1 and 2) was desalted to remove excess cross-linker and denatured by incubation at 65 °C for 15 min. The newly exposed sulfhydryl (-SH) groups on activase were then derivatized with 4 mM iodoacetamide at room temperature in the dark (Step 3). To allow enrichment and facilitate the identification of SH-containing peptides from the large pool of tryptic peptides (see below), a further derivatization with biotin_PEO before trypsin digestion, followed by avidin-agarose affinity purification, was performed (Steps 4–7). First, the iodoacetamide-derivatized activase was incubated with 8 mM DTT to reduce the native disulfide bonds in activase and the disulfide bond formed by PEAS derivatization followed by desalting to remove excess DTT (Step 4). Then, the newly released -SH groups were immediately derivatized by incubation with 10 mM biotin_PEO in the dark at room temperature for 2 h (Step 5). After removing excess biotin_PEO by desalting into 50 mM $NH_4HCO_3$ (pH 8.5), the samples were incubated with a sequencing grade trypsin modified by reductive methylation (Promega) at a 1:50 (w/w) ratio of protease/activase at 37 °C overnight (Step 6). To purify the biotin_PEO-derivatized peptides by avidin-agarose (Step 7), the beads (40 $\mu$l) were prepared first by incubating with biotin (1 mg/ml) to block the non-exchangeable biotin-binding sites. Then the agarose beads were washed with 20 bed volumes of 0.1 M glycine-HCl (pH 2.0) followed by an equilibration with 20 bed volumes of phosphate buffer (pH 7.4). The biotin_PEO-derivatized peptides were incubated with the equilibrated avidin-agarose at room temperature for 2 h. The beads were washed with 100 bed volumes of phosphate buffer (pH 7.4), and the bound peptides on avidin-agarose were eluted with biotin (1 mg/ml). Four fractions (100 $\mu$l) were collected. To increase the elution efficiency, the agarose beads were incubated for 20 min at room temperature in between each fraction.

*Mass Spectrometry*—Avidin-agarose purified tryptic fragments of Rubisco activase were first desalted on a high pressure liquid chromatography C18 reverse phase column (Vydac 218TP$^{TM}$) with $H_2O$/ACN to remove biotin and salts. Mass analysis was performed by using MALDI-TOF (Applied Biosystems Voyager-DE STR) (see Fig. 5*D*, *Step 8*). Before the mass analysis, the peptide samples were further desalted using C18 Zip-Tips (Millipore). Purified peptides were then mixed with an equal volume of $\alpha$-cyano-4-hydroxycinamic acid matrix solution (in 50% acetonitrile/0.1% trifluoroacetic acid) and subjected to mass spectrometry (Mass Spectrometry Laboratory at the University of Illinois). Mass spectra were taken by using the linear mode (30, 32).

*Immunoblot Assay*—Proteins were separated on 12% SDS-polyacrylamide gels and transferred onto polyvinylidene difluoride membranes. Membranes were incubated with primary antibodies against either spinach activase at dilution of 1:8000 or a synthesized 36-amino acid length of the C-terminal peptide (380–415; Fig. 1) of 46-kDa *Arabidopsis* activase at dilution of 1:4000. IRDye 700-labeled goat anti-rabbit secondary antibodies (LICOR, Lincoln, NE) were used at dilution of 1:10,000 or 1:20,000 (Rockland, Gilbertsville, PA). Visualization was accomplished by scanning the membranes with a LICOR Odyssey infrared image system (LICOR, Lincoln, NE), and bands were quantified with the Odyssey V1.2 application software.

## RESULTS

*Effects of Mutation of Negatively Charged Residues on the C-extension*—Six negatively charged residues (Glu$^{390}$, Asp$^{394}$, Glu$^{398}$, Asp$^{401}$, Asp$^{407}$, and Asp$^{408}$) are highly conserved (except Glu$^{398}$) and located near the two critical Cys residues (Cys$^{392}$ and Cys$^{411}$) on the C-extension of *Arabidopsis* 46-kDa isoform activase (Fig. 1). Alanine replacement of these negative residues was performed to examine their potential roles. Among the six single mutants, only E390A, D394A, and D401A exhibited ATP hydrolysis and Rubisco activation activities significantly higher than the recombinant wild type at an ADP/ATP ratio of 0.33 (data not shown). Two double mutants were then made to examine combined effects (Fig. 2, *A* and *B*). In the absence of ADP, the double mutants E390A/D401A and D394A/E398A had higher (2.3- and 1.8-fold, respectively) ATP hydrolysis and higher (2.2- and 1.7-fold, respectively) Rubisco activation activities than the wild type. At an ADP/ATP ratio of 0.33, a typical condition for the chloroplast stroma in the light, E390A/D401A was much less sensitive to ADP inhibition with 4.6-fold higher ATP hydrolysis and 6.6-fold higher Rubisco activation activities than the wild type. Replacement of D394A/E398A was less effective than E390A/D401A, resulting in 2.3-fold higher ATPase and 3.6-fold higher Rubisco activation activities than wild type at an ADP/ATP ratio of 0.33.

It is possible that the lower ADP sensitivity of the mutants is mainly due to an altered redox potential of the nearby cysteines. Therefore, the equilibrium redox midpoint potentials ($E_m$) for the ATP hydrolysis activity of the mutants E390A, D401A, and E390A/D401A were compared with the recombinant wild type

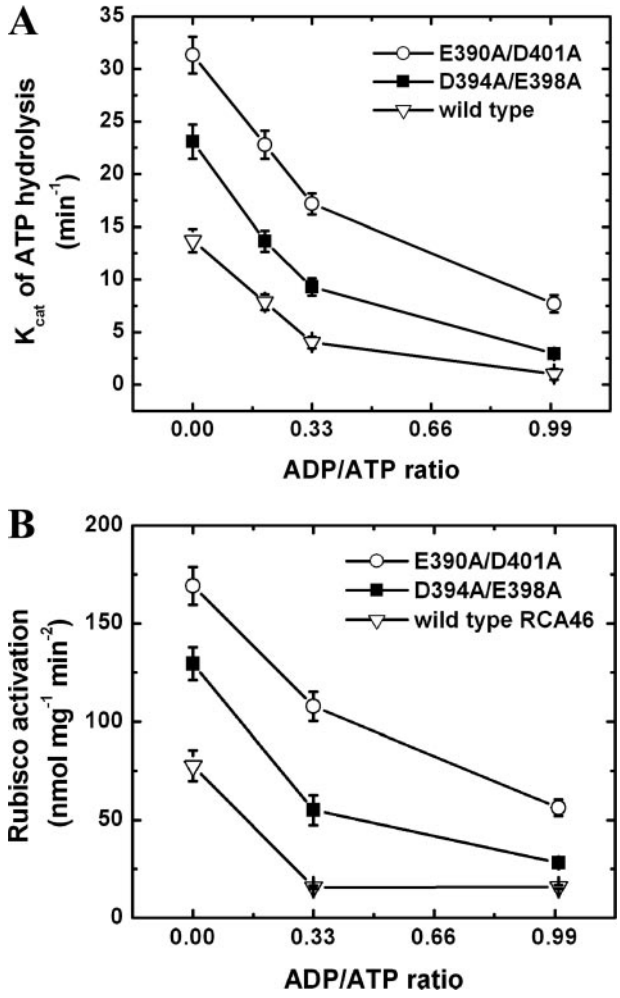


FIGURE 2. **ATP hydrolysis (*A*) and Rubisco activation activities (*B*) of activase at different ADP/ATP ratios.** Double mutants E390A/D401A (*open circles*) and D394A/E398A (*filled squares*) were compared with wild type (*open triangles*) 46-kDa isoform of activase. ATP hydrolysis activities were estimated by measuring the formation of inorganic phosphate from ATP. The Rubisco activation activity was assayed in an assay mixture (500 $\mu$l) containing 50 mM Tricine-KOH (pH 8.0), 20 mM $MgCl_2$, 0.1 mM EDTA, 4 mM RuBP, ATP, and ADP totaling 4 mM, 10 mM [$^{14}$C]$NaHCO_3$ (10 $\mu$Ci/ml), 75 $\mu$g of inactive Rubisco-RuBP complex, and 20 $\mu$g of activase. Rubisco activity was calculated from the difference in fixed $CO_2$ at successive time points. Rubisco activase activity corresponds to the increase in Rubisco activity with time.

enzyme at pH 7.9 as described previously (23). The redox titrations were all fitted by the Nernst equation for a single, two-electron component, with midpoint potentials very close to that of wild type (data not shown).

*Nucleotide Binding by Rubisco Activase*—Nucleotide binding by the recombinant wild type and mutant activase isoforms was compared by determining the apparent dissociation constants ($K_d$) for ADP and ATP$\gamma$S with 1-anilinonaphthalene-8-sulfonic acid fluorescence quenching (11, 12, 28). Binding of ATP$\gamma$S was also determined by intrinsic fluorescence enhancement as a function of nucleotide concentration (22). Binding of ATP was estimated from the concentration dependence ($K_m$) of ATP hydrolysis (22). After reduction by thioredoxin and DTT, the apparent dissociation constants ($K_d$) for ATP$\gamma$S and $K_m$ of ATP hydrolysis of the large (46-kDa) isoform decreased to 60 and 40% of those of the oxidized form, respectively, and thus became more similar to those of the small (43-kDa) isoform

**TABLE 1**

**The effects of redox changes and mutation on nucleotide binding capacities of wild type Rubisco activase**

The nucleotide binding of activase was estimated either using apparent dissociation constants ($K_d$) for ADP and ATP$\gamma$S by measuring fluorescence quenching of 1-anilinonaphthalene-8-sulfonic acid (ANS)/activase complex and intrinsic fluorescence increase of activase in response to different nucleotides concentration respectively or the ATP concentration for half maximal ATP hydrolysis activity of activase. RCA46ox and RCA46red represent the oxidized and reduced larger (46-kDa) isoform of *Arabidopsis* Rubisco activase respectively. C411A is Cys$^{411}$ to Ala mutant of the larger isoform. RCA43 represents the wild type smaller (43-kDa) isoform activase without any redox treatments.

| Rubisco activase | ANS fluorescence | | Intrinsic fluorescence ($K_d$-ATP$\gamma$S) | ATP hydrolysis ($K_m$) |
|---|---|---|---|---|
| | $K_d$-ADP | $K_d$-ATP$\gamma$S | | |
| | $\mu$M | $\mu$M | $\mu$M | $\mu$M |
| RCA46ox | 3.2 ± 0.2 | 15 ± 0.6 | 11 ± 0.4 | 135 ± 5 |
| RCA46red | 2.9 ± 0.1 | 9.3 ± 0.4 | 6.8 ± 0.3 | 54 ± 2 |
| C411A | 3.0 ± 0.2 | 9.1 ± 0.4 | 6.9 ± 0.3 | 58 ± 2 |
| E390A/D401A | 3.1 ± 0.2 | 9.4 ± 0.3 | 7.5 ± 0.3 | 79 ± 3 |
| RCA43 | 2.8 ± 0.1 | 7.4 ± 0.3 | 5.3 ± 0.2 | 28 ± 1 |

(Table 1). The observed effects of redox on ATP binding were somewhat less but otherwise consistent with a previous report (23). In contrast, the $K_d$ values for ADP of the small isoform and the reduced or oxidized large isoforms were all similar. These results indicate that redox modulation of the C-extension on the large isoform changes the affinity for ATP or its analog ATP$\gamma$S but not ADP. This conclusion is further supported by the observation that a C-terminal Cys-to-Ala mutant (C411A), which cannot be redox-modulated (13), also has a higher affinity for ATP (or ATP$\gamma$S) than the oxidized 46-kDa isoform. In addition, the double mutant (E390A/D401A) with decreased sensitivity to ADP inhibition (Fig. 2, *A* and *B*) also exhibited higher affinities for ATP and ATP$\gamma$S than the oxidized wild type 46-kDa isoform, with values more similar to the reduced 46-kDa isoform (Table 1). These results clearly indicate that the proper binding of ATP, but not ADP, in the nucleotide-binding pocket is selectively impaired only when the C-extension is oxidized and has negatively charged residues that might allow specific interactions with other residues near the nucleotide-binding domain.

*Sensitivity of C-extension to Proteolysis*—To demonstrate that conformational changes of the C-extension occur after redox treatments, sensitivity to a site-specific protease, thrombin, was compared between the reduced and oxidized forms of wild type 46-kDa activase (Fig. 3, *A* and *B*). Thrombin has only one cleavage site at $^{372}$GRG$^{374}$ (29) (Fig. 1) in the C-extension of the large isoform. The C-extension of the oxidized 46-kDa isoform remained almost intact after incubation with thrombin for 2 min, whereas 30% of the reduced isoform was cleaved to a 43-kDa band. A similar difference in sensitivity was observed at longer times of exposure. Immunoblots using antibody specific for the C-extension peptide (Fig. 3*A*) or whole enzyme (Fig. 3*B*) confirmed that the 43-kDa bands correspond to a C terminus-truncated form of 46-kDa activase. The redox treatments had no effect on the proteolytic activity of thrombin as measured by using a 48-kDa control protein (data not shown).

*Cysteine Insertion Mutation*—A new cysteine residue was inserted at position 402 (named C402$^{INS}$) in the C-extension of the 46-kDa isoform to examine the proximity of this domain to other regions of activase by chemical cross-linking. This approach has some similarities to previous studies that used the

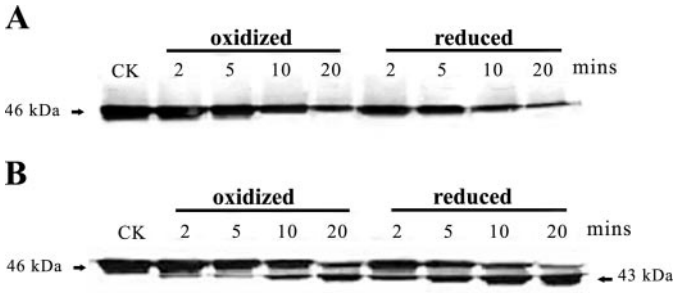


FIGURE 3. **Sensitivities of the reduced and oxidized large isoform of activase to proteolysis.** Conformational changes of the reduced and oxidized large isoform activase were detected by partial proteolysis using thrombin, a site-specific protease for the C-terminal extension. Wild type large isoform activase was incubated with thrombin for the indicated times after oxidation or reduction treatments. The sensitivity to proteolysis was analyzed by Western blots using an antibody raised against a C-terminal (36-amino acid) peptide (*A*) and an antibody raised against the full-length spinach activase (*B*). *CK* represents the control activase not exposed to thrombin.

**TABLE 2**

**ATP hydrolysis and Rubisco activation activities of the large 46-kDa isoform (wild type) and the C402$^{INS}$ insertion mutant before and after cross-linking**

ATP hydrolysis activities were measured by coupling ADP production to NADH oxidation. The Rubisco activation activity (nmol site min$^{-1}$) is calculated by dividing the observed increase in Rubisco activity with time by its maximal activity (2500 nmol min$^{-1}$ mg$^{-1}$), assuming 1 mg of Rubisco contains 14.3 nmol of active sites.

| Rubisco activase | ATP hydrolysis ($K_{cat}$) | Rubisco activation activity |
|---|---|---|
| | *min*$^{-1}$ | *nmol site min*$^{-1}$ *mg*$^{-1}$ |
| **Wild type** | 15 ± 1 | 5.7 ± 0.4 |
| **C402$^{INS}$ mutants** | | |
| Control[a] | 14 ± 1 | 5.7 ± 0.3 |
| PEAS_only[b] | 13 ± 1 | 5.6 ± 0.2 |
| UV_only[c] | 13 ± 1 | 5.5 ± 0.3 |
| −DTT[d] | 2.7 ± 0.2 | 1.3 ± 0.1 |
| +DTT[e] | 2.7 ± 0.2 | 1.4 ± 0.1 |

[a] Control, unmodified C402$^{INS}$.
[b] PEAS_only, PEAS-labeled C402$^{INS}$ only and no further treatments.
[c] UV_only, unmodified C402$^{INS}$ with 2-minute UV irradiation.
[d] −DTT, PEAS-labeled C402$^{INS}$ with 2-minute UV irradiation without DTT reduction.
[e] +DTT, PEAS-labeled C402$^{INS}$ with 2-minute UV irradiation followed by DTT reduction.

smaller isoform and exploits the observation that the endogenous cysteine residues (outside of the C-extension) are not very reactive (7, 24). In the absence of ADP, the C402$^{INS}$ mutant had ATP hydrolysis and Rubisco activation activities comparable with those of wild type 46-kDa activase (Table 2). The C402$^{INS}$ mutant exhibited a similar redox-dependent sensitivity to ADP as the wild type (Fig. 4). To examine whether the insertion mutation disturbs the formation of the disulfide bond between Cys$^{392}$ and Cys$^{411}$, the redox midpoint potential of C402$^{INS}$ was measured and found to be very close to that of wild type (data not shown).

*Cross-linking with the C402$^{INS}$ Mutant*—PEAS was selected as the cross-linker due to its shorter spacer arm (15 Å) *versus* a similar cross-linker *N*-(4-(p-azidosalicylamido) butyl)-3′(2′pyridyldithio) propionamide (Pierce) with a 21 Å arm. The successful application of PEAS for examining protein interactions has been reported previously (30–32). PEAS features a pyridyl disulfide group that can undergo disulfide exchange with thiol groups (Fig. 5*A*). An aryl azide on the other end of PEAS becomes activated upon exposure to UV light and reacts nonspecifically by forming a nitrene, which undergoes

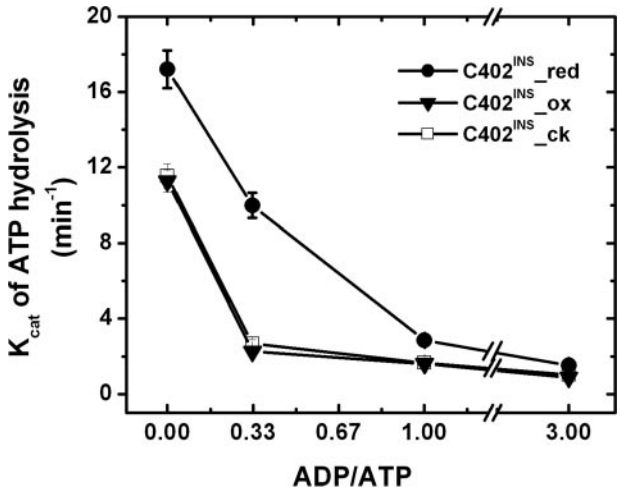


FIGURE 4. **ATP hydrolysis activity of the C402$^{INS}$ mutant at different ADP/ATP ratios after redox treatments.** ATP hydrolysis activities were estimated by measuring the formation of inorganic phosphate from ATP. C402$^{INS}$–red (*filled circles*) represents the Cys$^{402}$ insertion mutant of the large isoform activase reduced by thioredoxin-f and DTT. C402$^{INS}$–ox (*filled triangles*) represents the Cys$^{402}$ insertion mutant reoxidized by glutathione after a reduction treatment. C402$^{INS}$–ck (*open squares*) represents the Cys$^{402}$ insertion mutant without any treatments.

ring expansion and reacts with nearby nucleophiles (33). The cross-linked products can be released subsequently by cleavage of the disulfide bond introduced by PEAS modification with a reducing reagent to facilitate identification.

When PEAS-labeled C402$^{INS}$ was used for cross-linking, a prominent band corresponding to a cross-linked multimer of activase was observed in the absence of nucleotides and in the presence of ADP or ATP after 2 min of UV photo-activation (Fig. 5*B*). Less intense bands corresponding to cross-linked dimers and trimers of activase were also observed, particularly in the presence of ATP. The marked reduction in intensities (72% for no-nucleotides, 69% for ADP, and 41% for ATP after 2 min) of the 46-kDa bands indicate that extensive cross-linking between rather than within monomers occurred under all conditions. A prolonged (up to 10 min) UV irradiation did not significantly increase the cross-linking yields (data not shown). The cross-linking efficiency was very similar in the absence of nucleotides and in the presence of ADP but lower when ATP was present. Evidence of partial cross-linking between PEAS-labeled C402$^{INS}$ and non-modified wild type small (43-kDa) isoform activase was also observed when they were mixed at a 1:1 molar ratio (Fig. 5*C*). No apparent cross-linking products were detected when either wild type 43-kDa or wild type 46-kDa activase was used alone (data not shown).

ATP hydrolysis and Rubisco activation activity were measured before and after C402$^{INS}$ self-cross-linking (Table 2). UV photo-activation of PEAS-labeled C402$^{INS}$ abolished both its ATP hydrolysis and its Rubisco activation activities. Reduction by adding excess DTT after photo-activation did not recover the activities, although the higher ordered oligomers were almost completely converted into monomers (Fig. 5*B*). As a control, PEAS modification without UV irradiation or UV irradiation of unmodified enzyme had only minor effects on the activities of C402$^{INS}$.

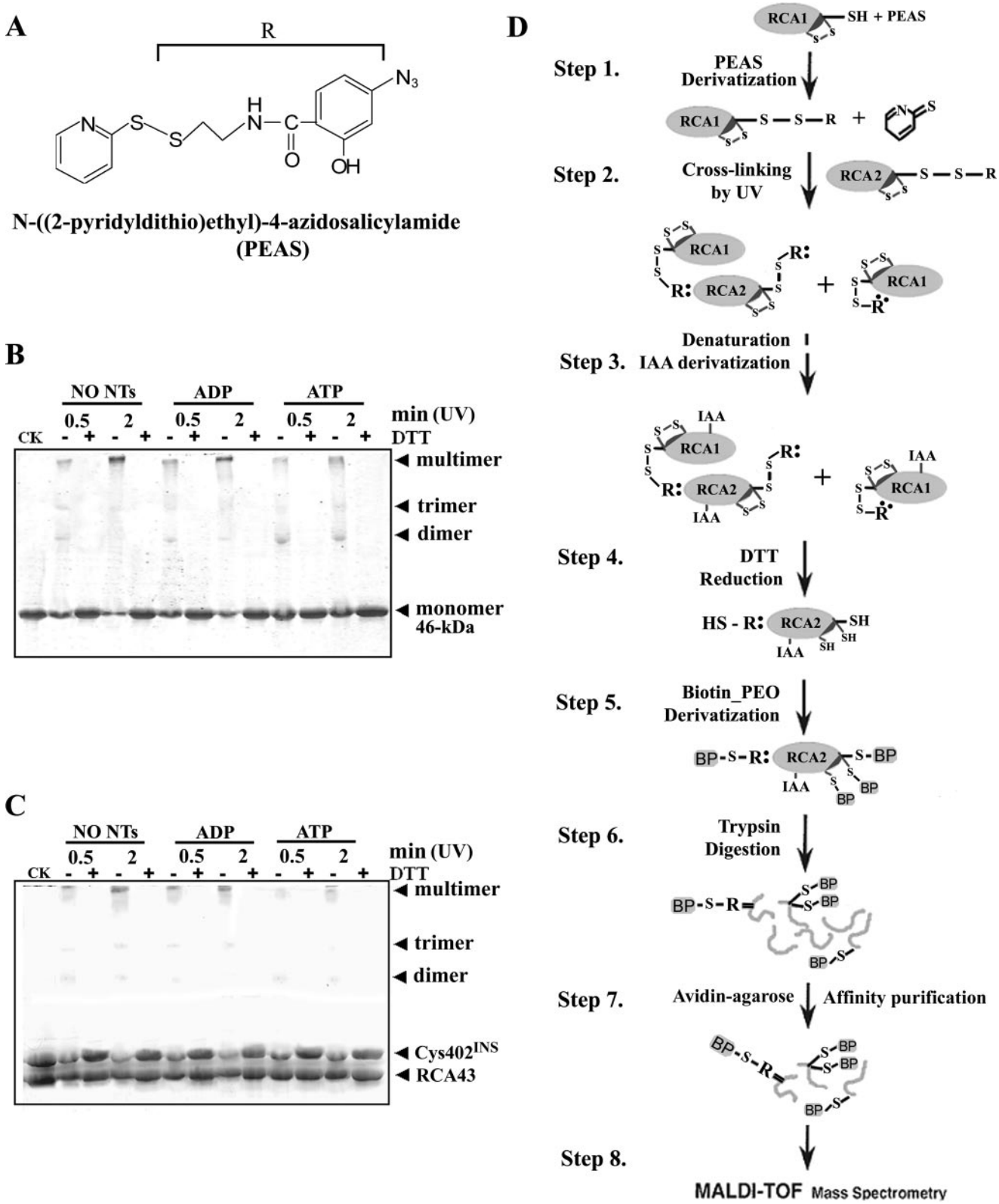


FIGURE 5. **Cross-linking with the C402$^{INS}$ insertion mutant.** A photo-activated, sulfhydryl-reactive cross-linker, PEAS, was used to modify the introduced cysteine in the oxidized form of the mutant (*A*). The PEAS-derivatized 46-kDa Cys$^{402}$ insertion mutant (C402$^{INS}$) was either self-cross-linked (*B*) or cross-linked with unmodified wild type 43-kDa activase (RCA43) (*C*) by irradiation with UV light for the indicated times. When cross-linking with RCA43, C402$^{INS}$ was first labeled with cross-linker reagent before mixing with RCA43 at a 1:1 molar ratio. Preincubation of activase with no nucleotides (*NO NTs*), ADP, or ATP was performed before cross-linking. The cross-linking efficiency was estimated by SDS-PAGE analysis under reduced (+*DTT*) and non-reduced (−*DTT*) conditions. A scheme for cross-linking and peptide identification is shown (*D*) in which *RCA1* and *RCA2* represent subunits of the C402$^{INS}$ mutant, *IAA* represents the derivatization by iodoacetamide, *BP* represents derivatization by biotin_PEO, and *R* is the moiety (*panel A*) that is transferred by disulfide exchange reaction to the sulfhydryl group of Cys$^{402}$ (see "Experimental Procedures" for details).

**A**

| No. | Exp. Mass | Peptide sequences (position) | Derivatization | Pred. Mass |
|---|---|---|---|---|
| 1 | 2846.2 | NFLTLPNIKVPLILGIWGGK (89-108) | PEAS/PEO_Biotin | 2845.8 |
| 2 | 2176.8 | VPLILGIWGGKGQGK (98-112) | PEAS/PEO_Biotin | 2175.7 |
| 3 | 1061.3 | MEK (241-243) | PEAS/PEO_Biotin | 1060.0 |
| 4 | 3702.0 | IKDEDIVTLVDQFPGQSIDFFGALRAR (266-292) | PEAS/PEO_Biotin | 3703.1 |
| 5 | 3300.8 | GAQQVNLPVPEGCTDPVAENFDCPTAR (380-406) | IAA/PEO_Biotin | 3300.8 |
| 6 | 3657.2 | GAQQVNLPVPEGCTDPVAENFDCPTAR (380-406) | PEO_Biotin | 3658.4 |
| 7 | 1536.9 | SDDGTCVYNF (407-416) | PEO_Biotin | 1536.0 |

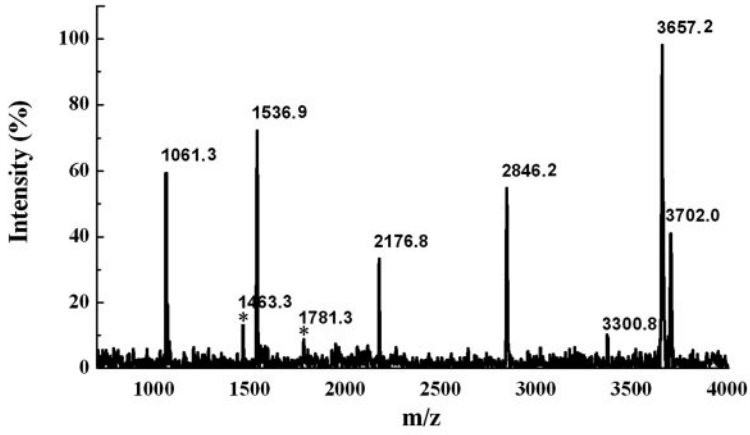


**B**

1 VKEDKQTDGD RWRGLAYDTS DDQQDITRGK GMVDSVFQAP MGTGTHHAVL SSYEYVSQGL

61 RQYNLDNMMD GFYIAPAFMD KLVVHITKNF LTLPNIKVPL ILGIWGGKGQ GKSFQCELVM

WALKER A

WALKER A WALKER B

121 AKMGINPIMM SAGELESGNA GEPAKLIRQR YREAADLIKK GKMCCLFIND LDAGAGRMGG

SENSOR I BOX VII

181 TTQYTVNNQM VNATLMNIAD NPTNVQLPGM YNKEENARVP IICTGNDFST LYAPLIRDGR

BOX VII BOX VII' SENSOR 2

241 MEKFYWAPTR EDRIGVCKGI FRTDKIKDED IVTLVDQFPG QSIDFFGALR ARVYDDEVRK

SENSOR 2

301 FVESLGVEKI GKRLVNSREG PPVFEQPEMT YEKLMEYGNM LVMEQENVKR VQLAETYLSQ

361 AALGDANADA IGRGTFYGKG AQQVNLPVPE GCTDPVAENF DCPTARSDDG TCVYNF

FIGURE 6. **MALDI analysis of biotin_PEO-derivatized tryptic peptides of the C402$^{INS}$ insertion mutant after cross-linking.** The sequences, experimental masses, and predicted masses (reported as $[M+H]^+$) of the derivatized peptides (*numbers 1–7*) enriched by affinity purification (see "Experimental Procedures" and Fig. 5*D*) are listed in order according to their positions in the amino acid sequence (*A*, *upper panel*). A representative mass spectrum is also shown (*A*, *lower panel*) in which peaks labeled with *asterisks* were unidentified. In *B*, the amino acid sequence of C402$^{INS}$ is shown with AAA$^+$ domains shaded in *gray*. Four peptides (*numbers 1–4*), which are identified as cross-linked with the C-terminal extension (*number 4* only appeared in one of three replicates), are *underlined* (*solid lines*). Peptides (*numbers 5–7*) that contain cysteine residue(s) were also recovered and indicated by *underlining* with *dashed lines*. Two native cysteines (Cys$^{392}$ and Cys$^{411}$) and one inserted cysteine (Cys$^{402}$) are marked with *asterisks* and an *arrow*, respectively.

*MALDI-TOF Identification of Sites Cross-linked to the C-extension*—Mass spectrophotometric analyses of peptides obtained with control and UV-irradiated PEAS-modified C402$^{INS}$ were inconclusive for clearly identifying modified peptides. Therefore, biotin_PEO derivatization and avidin-agarose affinity purification were used to isolate peptides containing only free -SH groups generated by reduction of either the endogenous disulfide bond in the oxidized activase or the disulfide bond introduced by PEAS modification. A representative mass spectrum of biotin_PEO-derivatized peptides of C402$^{INS}$ is shown in Fig. 6*A* (*lower panel*). A total of seven peaks observed in three independent replications are summarized in Fig. 6*A*, *upper panel*. Three peaks of particular interest are those with masses (reported as $[M+H]^+$) of 1061.3, 2176.8, and 2846.2 that correspond, respectively, to the peptides $^{241}$MEK$^{243}$ (adjacent to an Arg finger, Arg$^{240}$), $^{98}$VPLILGIWGGKGQGK$^{112}$ (P-loop), and ($^{89}$NFLTLPNIKVPLILGIWGGK$^{108}$ (P-loop) (Fig. 6*B*). Cross-linking to these peptides indicates that the introduced Cys (modified by PEAS) in the C-extension of oxidized C402$^{INS}$ is located near the nucleotide-binding pocket. A peak with *m*/*z* of 3702.0 corresponding to a peptide $^{266}$IKDEDIVTLVDQFPGQSIDFFGALRAR$^{292}$, which contains part of the Sensor 2 motif, was observed in one of three replications. Two peaks with *m*/*z* of 1536.9 and 3657.2 corresponding to a C-terminal peptide (407–416) containing Cys$^{411}$ and a peptide (380–406) containing Cys$^{392}$/Cys$^{402}$ were also observed. These peaks are attributed to biotin_PEO labeling of sulfhydryl groups formed from the Cys$^{392}$–Cys$^{411}$ disulfide bond by DTT reduction (Fig. 5*D*, *Steps 4* and *5*). A low signal peak with an *m*/*z* of 3300.8 matched the mass of a peptide 380–406 with one cysteine derivatized by iodoacetamide and another one by biotin_PEO, possibly due to incomplete formation of the disulfide bond between Cys$^{392}$ and Cys$^{411}$ in the starting material. Two additional small peaks marked with *asterisks* could not be identified.

## DISCUSSION

*The Roles of Conserved Negatively Charged Residues in the C-extension*—Our results show that the removal of negative charges contributed by Glu$^{390}$, Asp$^{394}$, and Asp$^{401}$ in the C-extension decreased the sensitivity of the large (46-kDa) isoform to ADP inhibition in a similar manner as observed with the Cys$^{392}$ and Cys$^{411}$ mutants (13) (Fig. 2, *A* and *B*). The similar redox midpoint potentials of the mutants and wild type (data not shown) indicate that the decreased ADP sensitivities of the mutants are not due to a disturbance in the formation of the nearby disulfide bond (Cys$^{392}$/Cys$^{411}$). In contrast, mutation of several polar or non-polar residues (Thr$^{410}$, Val$^{412}$, and Tyr$^{413}$) in the C-extension did not alter the redox regulation of the large isoform (23), suggesting a

special requirement for these negatively charged residues for redox regulation.

It was proposed that the negatively charged residues around $Cys^{392}$ and $Cys^{411}$ in the C-extension could stabilize a docking conformation that makes activase less accessible to ATP through electrostatic interactions with one or more positive residues on or close to the ATP-binding site (23). Consistent with this hypothesis, several positive residues ($Lys^{98}$, $Lys^{109}$, $Lys^{113}$, $Arg^{237}$, $Arg^{240}$, and $Lys^{243}$), of which $Lys^{113}$, $Arg^{237}$, $Arg^{240}$, and $Lys^{243}$ are essential for either ATP binding or ATP hydrolysis (4, 9, 10), are located on or immediately adjacent to the peptides cross-linked with the C-extension (Fig. 6). The elimination of probable ionic interactions in the $Glu^{390}$, $Asp^{394}$, and $Asp^{401}$ mutants will diminish any inhibitory interactions between the C-extension and the nucleotide-binding pocket. It is unlikely that $Glu^{390}$, $Asp^{394}$, and $Asp^{401}$ interact with $Mg^{2+}$ in a similar manner as an aspartate residue ($Asp^{170}$ in *Arabidopsis* activase) in Walker B (7) because the removal of negative charges on $Glu^{390}$ and $Asp^{401}$ increased the affinities for ATP (1.7-fold) and ATPγS (1.6-fold) in contrast to the Asp-to-Ala mutant in Walker B with a decreased (13.7-fold) affinity for ATP in the presence of $Mg^{2+}$ (7, Table 1).

*Redox-mediated Conformational Change of the C-extension*—Our observation of redox-dependent sensitivities of the C-extension to proteolysis supports the proposal that conformational changes of the C-extension occur as part of its redox regulatory role in altering the response to the ADP/ATP ratio (23) (Fig. 3). One interpretation consistent with the other data is that formation (or reduction) of a disulfide bond is accompanied by a conformational change that docks (or removes) the C-extension into (or from) the nucleotide-binding pocket, which alters the access of thrombin to the proteolysis site. In fact, a similar mechanism has been confirmed in oxidized sorghum NADP-malate dehydrogenase, which is redox-regulated in chloroplast (34, 35). A three-dimensional structure of NADP-malate dehydrogenase clearly shows that formation of a disulfide bond between two carboxyl cysteine residues ($Cys^{365}$/$Cys^{377}$) results in folding of the inhibitory C-terminal peptide into the active sites.

*The C-extension of Oxidized 46-kDa Activase Is in Close Proximity to the Nucleotide-binding Pocket*—Our cross-linking studies provide strong evidence for the proposal that the C-extension of the oxidized large isoform is located near the ATP-binding site (23). First, three peptides ($Asn^{89}$–$Lys^{108}$, $Val^{98}$–$Lys^{112}$, and $Met^{241}$–$Lys^{243}$), cross-linked with the C-extension of the oxidized PEAS-labeled $C402^{INS}$ mutant of the 46-kDa activase, are located in the subdomains of the nucleotide-binding pocket (1) (Fig. 6*B*). The first two are part of a Walker A (P-loop) directly involved in nucleotide binding (4, 5, 36). The third peptide, located in Box VII, contains one of the three residues ($Arg^{237}$, $Arg^{240}$, and $Lys^{243}$) that are essential for ATP hydrolysis but not for ATP binding and may interact with the γ-phosphate of ATP (9, 11). Second, the cross-linking of the PEAS-labeled C-extension significantly lowered the both ATPase and Rubisco activation activities of oxidized $C402^{INS}$ (Table 2), which is in sharp contrast to the observation (24) that cross-linking between the N and C termini of the small activase isoform doubled its ATPase activity. Therefore, we conclude that the close proximity (15 Å) of the C-extension on the oxidized large isoform to the nucleotide-binding pocket accounts for its redox regulatory effects.

Furthermore, the extensive intersubunit cross-linking observed with the $C402^{INS}$ mutant (Fig. 5*B*) is consistent with the conclusion that the nucleotide-binding pocket in many AAA proteins usually consists of residues from adjacent subunits in oligomeric assemblies (3, 37). Also, the partial intersubunit cross-linking observed when the $C402^{INS}$ mutant and wild type small (43-kDa) isoform were mixed (Fig. 5*C*) suggests that the interactions between the two isoforms include the C-extension. Such an interaction may explain how the larger isoform can regulate both isoforms *in vitro* and *in vivo* (13, 14) but will need further investigation.

*Selective Interference of the C-extension with ATP Hydrolysis*—A comparison of nucleotide affinities between the oxidized and reduced large isoforms suggests that the C-extension of the oxidized isoform selectively interferes with ATP (but not ADP) binding and ATP hydrolysis (Table 1). Two other observations support this conclusion. First, the cross-linking efficiency of $C402^{INS}$ was much lower in the presence of ATP than ADP or no nucleotides, which suggests a competitive binding between the C-extension and ATP but not ADP (Fig. 5, *B* and *C*). Second, the C-extension was cross-linked to a peptide in the Box VII region, which contains residues that are required for ATP hydrolysis but not nucleotide binding (7, 9) (Fig. 6). The latter observation could be important for understanding how small differences in nucleotide binding (1.1-fold for ADP and 2.5-fold for ATP) between the oxidized and reduced large isoform of activase are accompanied by a nearly 10-fold difference in ATP hydrolysis activity at an ADP/ATP ratio of 1:3 (13, Table 1).

Based on the results reported here and previous research on the redox modulation of activase, we conclude that the C-extension of the oxidized 46-kDa isoform of activase locates in close proximity to the nucleotide-binding pocket and thereby plays an inhibitory role in ATP hydrolysis that is regulated by redox. Formation of a disulfide bond between $Cys^{392}$ and $Cys^{411}$, the presence of the negatively charged residues ($Asp^{390}$, $Glu^{394}$, and $Asp^{401}$), and the redox-dependent conformational changes of the C-extension, which position it near the nucleotide-binding pocket, all combine to alter the sensitivity of activase to ADP inhibition. Thus these studies provide new insights into the mechanism of redox regulation of activase by the C-extension in the large isoform.

*Acknowledgment—We thank Dr. S. C. Huber (U. S. Department of Agriculture-Agricultural Research Service) for allowing access to the LICOR Odyssey infrared image system.*

## REFERENCES

1. Portis, A. R., Jr. (2003) *Photosynth. Res.* **75,** 11–27
2. Robinson, S. P., and Portis, A. R., Jr. (1989) *Arch. Biochem. Biophys.* **268,** 93–99
3. Neuwald, A. F., Aravind, L., Spouge, J. L., and Koonin, E. V. (1999) *Genome. Res.* **9,** 27–43
4. Shen, J. B., Orozco, E. M., and Ogren, W. L. (1991) *J. Biol. Chem.* **266,** 8963–8968
5. Shen, J. B., and Ogren, W. L. (1992) *Plant Physiol.* **99,** 1201–1207

6. Salvucci, M. E., Rajagopalan, K., Sievert, G., Haley, B. E., and Watt, D. S. (1993) *J. Biol. Chem.* **268,** 14239–14244
7. van de Loo, F. J., and Salvucci, M. E. (1998) *Biochemistry* **37,** 4621–4625
8. Li, C., Salvucci, M. E., and Portis, A. R., Jr. (2005) *J. Biol. Chem.* **280,** 24864–24869
9. Li, C., Wang, D., and Portis, A. R., Jr. (2006) *Arch. Biochem. Biophys.* **450,** 176–182
10. Salvucci, M. E., and Klein, R. R. (1994) *Arch. Biochem. Biophys.* **314,** 178–185
11. van de Loo, F. J., and Salvucci, M. E. (1996) *Biochemistry* **35,** 8143–8148
12. Wang, D., and Portis, A. R., Jr. (2006) *Photosynth. Res.* **88,** 185–193
13. Zhang, N., and Portis, A. R., Jr. (1999) *Proc. Natl. Acad. Sci. U. S. A.* **96,** 9438–9443
14. Zhang, N., Kallis, R. P., Ewy, R. G., and Portis, A. R., Jr. (2002) *Proc. Natl. Acad. Sci. U. S. A.* **99,** 3330–3334
15. Werneke, J. M., Chatfield, J. M., and Ogren, W. L. (1989) *Plant Cell* **1,** 815–825
16. Rundle, S. J., and Zielinski, R. E. (1991) *J. Biol. Chem.* **266,** 4677–4685
17. To, K. Y., Suen, D. F., and Chen, S.-C. G. (1999) *Planta* **209,** 66–76
18. Zhang, Z. L., and Komatsu, S. (2000) *J. Biochem.* **128,** 383–389
19. Salvucci, M. E., van de Loo, F. J., and Stecher, D. (2003) *Planta* **216,** 736–744
20. Salvucci, M. E. (1992) *Arch. Biochem. Biophys.* **298,** 688–696
21. Wang, Z. Y., Ramage, R. T., and Portis, A. R., Jr. (1993) *Biochim. Biophys. Acta* **1202,** 47–55
22. Lilley, R. M., and Portis, A. R., Jr. (1997) *Plant Physiol.* **114,** 605–613
23. Zhang, N., Schürmann, P., and Portis, A. R., Jr. (2001) *Photosynth. Res.* **68,** 29–37
24. Salvucci, M. E. (2004) *FEBS Lett.* **560,** 205–209
25. Schürmann, P., and Jacquot, J. P. (2000) *Plant Mol. Biol.* **51,** 371–400
26. Wang, Z. Y., and Portis, A. R., Jr. (1992) *Plant Physiol.* **99,** 1348–1353
27. Kallis, R. P., Ewy, R. G., and Portis, A. R., Jr. (2000) *Plant Physiol.* **123,** 1077–1086
28. Wang, Z. Y., and Portis, A. R., Jr. (1991) *Biochim. Biophys. Acta* **1079,** 263–267
29. Keil, B. (1992) *Specificity of Proteolysis*, pp. 335, Springer-Verlag New York Inc., New York
30. Cai, K., Itoh, Y., and Khorana, H. G. (2001) *Proc. Natl. Acad. Sci. U. S. A.* **98,** 4877–4882
31. Pioszak, A. A., Jiang, P., and Ninfa, A. J. (2000) *Biochemistry* **39,** 13450–13461
32. Itoh, Y., Cai, K., and Khorana, H. G. (2001) *Proc. Natl. Acad. Sci. U. S. A.* **98,** 4883–4887
33. Schuster, G. B., and Platz, M. S. (1992) *Adv. Photochem.* **17,** 69–143
34. Ruelland, E., Johansson, K., Decottignies, P., Djukic, N., and Miginiac-Maslow, M. (1998) *J. Biol. Chem.* **273,** 33482–33488
35. Johansson, K., Ramaswany, S., Saarinen, M., Lemaire-Chamley, M., Issaki-dis-Bourguet, E., Miginiac-Maslow, M., and Eklund, H. (1999) *Biochemistry* **38,** 4319–4326
36. Walker, J. E., Saraste, M., Runswick, M. J., and Gay, N. J. (1982) *EMBO J.* **1,** 945–951
37. Ogura, T., and Wilkinson, A. J. (2001) *Genes Cells* **6,** 575–597